

## TrackFly: Virtual reality for a behavioral system analysis in free-flying fruit flies

Steven N. Fry<sup>a,b,\*</sup>, Nicola Rohrseitz<sup>b</sup>, Andrew D. Straw<sup>c</sup>, Michael H. Dickinson<sup>c</sup>

<sup>a</sup> Institute of Robotics and Intelligent Systems, ETH Zürich, Switzerland

<sup>b</sup> Institute of Neuroinformatics, ETH/University of Zürich, Switzerland

<sup>c</sup> California Institute of Technology, Pasadena CA, USA

### ARTICLE INFO

#### Article history:

Received 25 January 2008

Received in revised form 22 February 2008

Accepted 26 February 2008

#### Keywords:

Virtual reality

Tracking

Insects

*Drosophila*

Vision

Behavior

Flight

Control

### ABSTRACT

Modern neuroscience and the interest in biomimetic control design demand increasingly sophisticated experimental techniques that can be applied in freely moving animals under realistic behavioral conditions. To explore sensorimotor flight control mechanisms in free-flying fruit flies (*Drosophila melanogaster*), we equipped a wind tunnel with a Virtual Reality (VR) display system based on standard digital hardware and a 3D path tracking system. We demonstrate the experimental power of this approach by example of a 'one-parameter open loop' testing paradigm. It provided (1) a straightforward measure of transient responses in presence of open loop visual stimulation; (2) high data throughput and standardized measurement conditions from process automation; and (3) simplified data analysis due to well-defined testing conditions.

Being based on standard hardware and software techniques, our methods provide an affordable, easy to replicate and general solution for a broad range of behavioral applications in freely moving animals. Particular relevance for advanced behavioral research tools originates from the need to perform detailed behavioral analyses in genetically modified organisms and animal models for disease research.

© 2008 Elsevier B.V. All rights reserved.

### 1. Introduction

A detailed understanding of how animals control their movements in a complex natural environment is likewise relevant to neuroscientists exploring neuromotor control mechanisms and engineers attempting to implement biological control principles in microrobots, such as micro air vehicles (MAVs). The reflexive flight control mechanisms of insects are experimentally highly amenable and therefore serve as powerful model systems to explore neuromotor control mechanisms (e.g. Frye and Dickinson, 2001).

Here we describe methods developed for a detailed behavioral system analysis in freely flying fruit flies (*Drosophila melanogaster* Meigen). Based on Virtual Reality (VR) display techniques implemented in standard digital hardware, we designed an automated 'one-parameter open loop' testing paradigm that allowed us to quantify the open loop transfer properties of the fly's visual ground speed response. The ability to perform meaningful behavioral analyses with a high throughput meets the demands for an interdisciplinary research effort on neuromotor control strategies based on

advanced genetic tools and concepts derived from control systems engineering.

#### 1.1. Open loop stimulation in tethered insects

The mechanisms underlying visuomotor flight control, like most other behaviors, are highly complex. This complexity can be approached with a reductionist approach, in which the animal is considered as a system of interconnected control loops, which can be analyzed using standard control system analysis techniques. In this approach, various sensory modalities are considered as inputs to the system, which after a sensorimotor transduction process lead to the motor output. As a result of the interaction with the physical environment, this leads to appropriate behavior and consequently generates sensory feedback, closing the feedback control loop (Fig. 1).

In the past, visuomotor flight control mechanisms of flies and other insects have been explored extensively under restricted experimental conditions. As a classic approach, input–output relationships of identified neuromotor control loops have been measured from rigidly tethered insects, in which sensory stimuli can be delivered precisely and the resulting motor output measured with comparatively simple tools. As a result, it has been possible to characterize sensorimotor systems from their transfer properties, allowing structure–function relationships to be inferred. In the bio-

\* Corresponding author at: Institute of Neuroinformatics, ETH Zürich, Winterthurerstrasse 190, CH-8057 Zürich, Switzerland. Tel.: +41 44 635 30 45; fax: +41 44 635 30 53.

E-mail address: [steven@ini.ch](mailto:steven@ini.ch) (S.N. Fry).

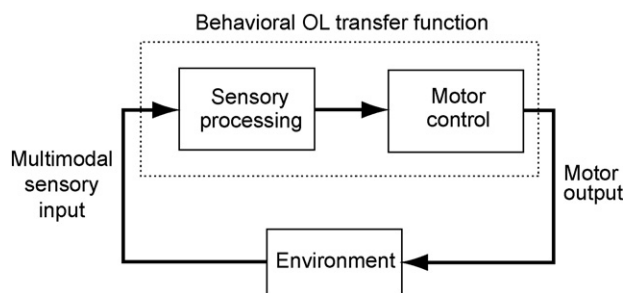


**Fig. 1.** General scheme of sensorimotor flight control. The relationship between sensory input and motor output is measured directly using an open loop paradigm. In the naturally behaving animal, the sensory input is reafferently coupled to the motor output (closed loop condition).

logical literature the stimulus condition is referred to as *open loop* to reflect the experimental de-coupling of the sensory stimulus from the motor behavior.

Countless combinations of sensory stimulation and recording of motor actions have been employed alone in flies, including for example: leg extension elicited from optic flow (Borst and Bahde, 1986), head movements from visual or mechanical stimulation (Hengstenberg et al., 1986), walking behavior in presence of visual cues (Götz and Wenking, 1973), flight behavior in presence of varying visual (Götz, 1964, 1965, 1968; Blondeau, 1981; reviews: Buchner, 1984; Collett et al., 1993), olfactory (Frye and Dickinson, 2004) or wind (Gewecke, 1967) stimuli.

Examples of open loop experiments in other species include acoustic target tracking in crickets (e.g. Hoy and Paul, 1973; Hedwig and Poulet, 2004; for recent methods see Lott et al., 2007), optomotor (Baader, 1991) and object avoidance responses (Robertson and Johnson, 1993) in tethered flying locusts.

### 1.2. Limitations of tethered preparations

While tethered paradigms offer a broad range of powerful experimental possibilities, their significance for realistic behavior is limited due to the significant inconsistencies between natural and experimental conditions (discussed, e.g. in Buchner, 1984; Gray et al., 2002; Taylor and Zbikowski, 2005). Flies, for example, rely on mechanosensory feedback from specialized balance organs, the halteres (Pringle, 1984; Nalbach and Hengstenberg, 1994) for flight stabilization and bilateral haltere ablation indeed renders the fly incapable of stable flight (Derham, 1714, cited by Dickinson, 2005). Tethering disrupts the reafferent mechanical input to the halteres and tethered flies accordingly show strong behavioral artifacts, including distorted wing stroke kinematics (Fry et al., 2005) and a several-fold prolonged time course of turning maneuvers in visual flight simulators (Heisenberg and Wolf, 1979). Though realistic flight dynamics can be experimentally implemented at least partially with loose tethers (e.g. Baker, 1979; Heisenberg and Wolf, 1979; Mayer et al., 1988; Bender and Dickinson, 2006), a meaningful analysis of neuromotor flight control mechanisms ultimately requires behavioral data to be measured in flies flying freely under realistic flight conditions (e.g. *Drosophila*: Fry et al., 2003; *Fannia*: Land and Collett, 1974).

### 1.3. Motivation for a one-parameter open loop, free-flight paradigm

Numerous behavioral studies performed in freely flying insects have addressed sensorimotor control mechanisms (reviews: Collett et al., 1993; Srinivasan and Zhang, 2004), and visual flight speed responses of various insect species in particular (e.g. mosquito: Kennedy, 1939; moth: Willis and Arbas, 1991; bee: Srinivasan et al.,

1996; fly: David, 1979). Previous studies of visual speed control in free-flying insects showed that insects maintain a 'preferred' flight speed relative to the visual surround, irrespective of the pattern's spatial frequency (David, 1982; Srinivasan et al., 1996).

To explore the control properties of the flight speed response, it was necessary to stimulate flies with *arbitrary* visual patterns over a broad parameter range and measure the resulting corrective responses. Furthermore, the measurement of transient responses is essential to a formulation of time-continuous models, as presented elsewhere (Rohrseitz and Fry, in preparation).

To this end, we implemented a free flight, 'one-parameter open loop' paradigm using a wind tunnel equipped with Virtual Reality display technology. Our methods allowed fully automated mass testing of individual flies over a broad range of visual stimuli, combining the advantages of open loop visual stimulation with the advantages of performing behavioral experiments under realistic free flight conditions (see Schuster et al., 2002, for a comparable approach in walking fruit flies). Furthermore, our methods allowed a straightforward implementation of various other behavioral paradigms, including the presentation of virtual objects, Gabor patches and naturalistic images.

## 2. Experimental system

### 2.1. Wind tunnel

The behavioral tests were performed in a commercial open circuit, closed throat wind tunnel (Engineering Laboratory Design, Inc., Lake City, MN, USA), equipped with a real time 3D tracking system and virtual reality display technology (Fig. 2 and see below). The wind tunnel provided a laminar airflow in a working section made of clear acrylic, 1.55 m in length and 0.305 m in width and height. Standard tests were performed using a wind speed of  $0.37 \text{ m s}^{-1}$ . An attractant odor ('Kressi' herb vinegar, diluted to 5% solution) was vaporized using an ultrasonic humidifier (Boneco) at a rate of approximately  $7.2 \text{ mg s}^{-1}$  from 4 nozzles positioned in front of the air intake end of the wind tunnel. Control tests using an odor–smoke mixture confirmed a homogeneous dispersion of the

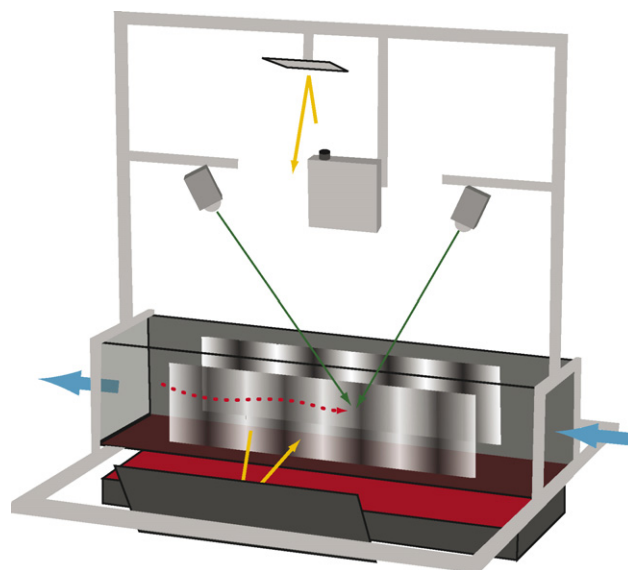


**Fig. 2.** Free flight experimental setup. A wind tunnel was equipped with a real time 3D position tracking system (Trackit 3D, Fry et al., 2000, 2004) and custom-programmed graphical rendering software (based on the VisionEgg, Straw and O'Carroll, 2003; Straw et al., 2006). Visual stimuli were presented in open loop to free-flying flies by compensating for their position along the wind tunnel in real time.

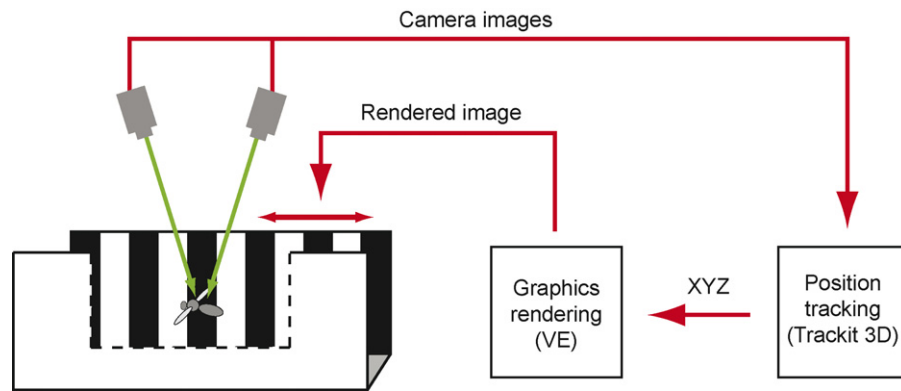


**Fig. 3.** Virtual reality display configuration. The fly's 3D position is measured (delay:  $\sim 18$  ms) using Trackit 3D and two standard PAL video cameras. The position data ("XYZ") are transferred to a client PC via a network interface and used to render and display an image on the wind tunnel's side walls (delay:  $\sim 19 \pm 8$  ms).

odor within the laminar airflow. While the presence of odor likely increased the flies' motivation to track up wind, it did not provide directional cues for up wind tracking as would have been the case with an odor plume or gradient.

Fruit flies (*D. melanogaster*) were reared in the laboratory using standard procedures. 2–4-day-old male and female flies were isolated and deprived of food, but not water, during 12–16 h prior to an experiment. A few flies at a time were released into the wind tunnel through a Plexiglas tube at the downwind end of the wind tunnel, where they voluntarily initiated upwind flight.

## 2.2. Real time flight path tracking

Flies were tracked in real time using Trackit 3D (Bioobserve GmbH, Bonn, Germany), also see (Fry et al., 2004), on a standard personal computer (CPU: 1.1 GHz) running Microsoft Windows 2000 SP4). Trackit 3D was equipped with two Sony LSX-PT1 color video cameras, whose infrared filters were removed for increased sensitivity in the long wave spectrum. The cameras filmed the flies from above against a bright homogeneous background, provided from a custom built lamp attached below the working section. The lamp contained 10 dimmable high-frequency luminescent tubes (Osram Lumlux, Daylight 36W connected to Feller, 230 VAC, 50 Hz dimmers) covered with translucent red Plexiglas (Transsatco, red 8%). The fruit flies were not distracted by the light shining from below because of their low sensitivity in the long wavelength spectrum (Heisenberg and Buchner, 1977; Stark and Johnson, 1980).

The three-dimensional position of single flies, measured at 50 Hz, was transferred to a client computer with a short latency (see Section 2.4) using a TCP/IP (Transmission Control Protocol/Internet Protocol) network interface (Fig. 3).

## 2.3. Image rendering and display

Custom software was developed in Python (version 2.4) to render the visual stimulus on a client computer (CPU: AMD Athlon, 1.9GHz; Operating System: Microsoft Windows 2000, Service Pack 4; graphics Card: Asus V9520 Magic/T/128 with a NVIDIA GeForce FX 5200 chip set) in real time. An asynchronous loop was used to query the network port for the last measured position of the fly using the custom programmed Python module PyTrackit ([www.visionegg.org](http://www.visionegg.org)). Based on the position information, an appropriate stimulus was rendered using the open source graphic library, The VisionEgg (version 1.0; [www.visionegg.org](http://www.visionegg.org); Straw and O'Carroll, 2003; Straw et al., 2006), which supports the OpenGL hardware acceleration features of standard graphic cards. Finally, the fly's position and stimulus conditions were logged to a data file for later analysis.

### 2.3.1. Spatial properties

The image was displayed using a LCD (liquid crystal display) projector (Sony, VPL-ES1). The image was split with a pair of angled mirrors and projected via a pair of large mirrors onto tracing paper screens ( $1.0 \text{ m} \times 0.3 \text{ m}$ ) attached to the side walls of the wind tunnel (Fig. 2). Image distortion resulting from the projection system was corrected in the software at the level of image rendering. The distortion parameters were measured using a calibration procedure, in which a virtual display was projected and adjusted to the physical display. The calibration resulted in a rendering resolution of 1 mm. With a full-screen image resolution of 800 pixels  $\times$  600 pixels, the maximal angular separation of the pixels in the middle of the wind tunnel was  $0.38^\circ$  and therefore well below the fruit fly's spatial cut-off frequency of  $9.4^\circ$  (Götz, 1964).

### 2.3.2. Luminance

To ensure that the luminance values defined in the software were faithfully represented on the display screens, we created a gamma lookup table that produced a linear relation between specified pixel values and the screen luminance, which we measured using a photodiode. To maximize the luminance visible to the fly, we stimulated using the green and blue, but not the red color channel (also see Section 2.2). Maximum luminance and Michelson contrast,  $(I_{\text{Max}} - I_{\text{Min}})/(I_{\text{Max}} + I_{\text{Min}})$  were measured at  $20.9 \text{ Cd m}^{-2}$  and 0.56, respectively.

### 2.3.3. Temporal properties

The temporal display properties are of particular importance when considering experiments with visual motion stimuli. Display systems susceptible to flicker at frequencies perceptible to the visual system are generally avoided for visual studies. For experiments in insects this precludes the use of CRT (cathode ray tube) displays with standard refresh rates up to about 120 Hz, a value below the temporal resolution limit of flies (Juusola and Hardie, 2001). We avoided using a projector based on digital light processing (DLP) technology, which typically produces strong luminance modulations, albeit at relatively high frequencies. Conversely, liquid crystal display projectors are susceptible only to the luminance fluctuations of the light source. To avoid undesired side effects, we chose a LCD projector that showed no measurable variance in luminance when displaying a static image.

Artifacts could also result from the discretized representation of motion resulting from the finite refresh rate of the display. With a standard native refresh rate of 60 Hz typical for LCD projectors and temporal frequencies of displayed sine grating stimuli typically up to about  $10 \text{ s}^{-1}$ , the transition of one pattern period was represented by 6 discrete positions. In the behaviorally more relevant range of about  $5 \text{ s}^{-1}$  this value is increased above 10 positions

per cycle. Though the discretized representation of moving gratings remains limited, electrophysiological experiments on visual interneurons revealed substantial tolerance to temporal aliasing (Straw and O'Carroll, 2003).

A further limitation of the display lies in the response time of LCD displays, which could result in blurring of moving objects. To test for possible image degradation due to non-linear temporal response characteristics of the LCD projector, we tested the temporal profile of displayed moving sine gratings using a photodiode. We found that the locally measured temporal luminance waveform remained sinusoidal and undiminished in amplitude within the parameter range used in the experiments (data not shown).

#### 2.4. Closed loop system latency

We define the closed loop system latency as the time lag between the sampling of the fly's position by the cameras and the update of the display as a result of this position measurement. This time lag is composed of the time required: (1) by Trackit 3D to send a position message after the image of the fly was sampled by the cameras, and (2) the image rendering system to render an image according to the measured fly's 3D position. We measured the first latency from the time required by Trackit 3D to register the position of a triggered light emitting diode (LED) and sending a signal to the computer's parallel port (which itself has a negligible latency in the order of microseconds) at a near constant 0.018 s. We then measured the second latency from the time passed between the measurement of the fly's position and displaying the image on the screen. The update of the asynchronously rendered display depended on the screen location, averaging at 0.019 s (min: 0.012 s, max: 0.027 s). The total system latency for the average screen location therefore lay at around  $\tau = 0.038$  s.

Though the pattern phase lag resulted in a 10% error of stimulus magnitude in our experimental paradigm, this error was consistent and could easily be accounted for in the data analysis, and therefore did not compromise the validity of the experimental procedure (see Section 3.4.2 for more details). In a different paradigm,

however, shorter time lags might be required. Using standard hardware, 200 Hz position tracking and 300 Hz displays are currently feasible and could reduce the system latency several-fold. As the computational power of digital technology is quickly increasing, possible remaining hardware limitations will tend to be reduced in the future.

#### 2.5. Coordinate system

Numerous studies employed periodic physical patterns to induce visual responses in free-flying insects (see Introduction). We have reproduced this experimental condition by projecting sine gratings on the side walls of the wind tunnel (Figs. 2–4A; note sine gratings are represented by stripes for simplicity; +X denotes up wind direction). The stimulus is defined by its spatial frequency (SF, the number of cycles per unit length of the visual display; unit:  $\text{m}^{-1}$ ), its temporal frequency (TF, the number of cycles passing a given point of the display per unit time, unit:  $\text{s}^{-1}$ ; positive up wind), as well as its luminance. Pattern period  $\Delta$  is calculated from  $1/\text{SF}$  (unit: m).

From the fly's perspective, objects appear the largest in a lateral position and progressively smaller toward more frontal and caudal azimuths due to geometric distortion. Concomitantly, objects reach their maximum angular velocity ( $\text{degree s}^{-1}$ ) as they pass the fly laterally. Geometric distortion applies likewise for elevation. Note use of capitalized and non-capitalized symbols for linear and angular metrics, respectively.

To stimulate flies with a single retinal pattern period, we also displayed distorted sine grating patterns, by transforming the frame of reference of the wind tunnel from cartesian to cylindrical, as if projecting the planar pattern onto a virtual drum centered on the fly (Fig. 4B). We achieved the distortion using

$$I = I_0 \cdot \sin(2\pi(t \cdot \text{TF} + \alpha \cdot \text{sf})) + I_m, \quad (1)$$

with

$$\alpha = a \tan\left(\frac{x}{\omega/2}\right) \quad (2)$$

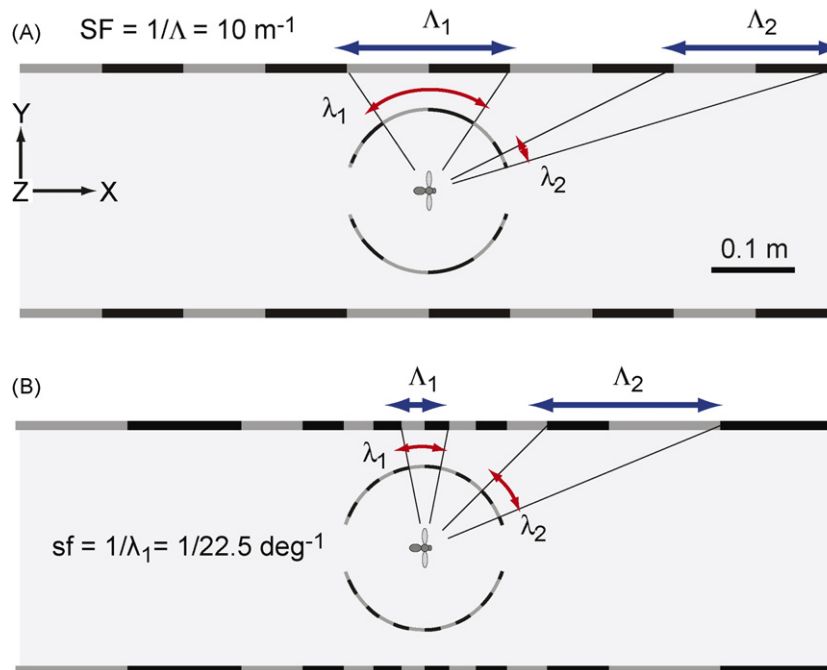


**Fig. 4.** Coordinate systems with wind tunnel shown from above. (A) Constant linear spatial frequency. The spatial pattern period as displayed on the screen ( $\Delta$ , m) is constant. The angular pattern period as projected on the eye ( $\lambda$ ,  $^\circ$ ) decreases toward frontal and caudal positions. (B) Virtual "drum" display. The pattern is distorted such that a constant angular spatial wavelength is obtained for all azimuthal positions.

$I_0 = I_m = 0.5$ . Although the stimulus conditions generated in this way are highly unnatural, the stimulus conditions were nevertheless useful to test specific questions relating to visual motion processing mechanisms underlying the measured responses (Rohrseitz and Fry, in preparation).

### 3. Experiments

#### 3.1. Overview

As an application example, we describe the implementation of an automated, 'one-parameter open loop' testing paradigm, which was used to explore the dynamics of visual flight speed control in the fruit fly. An automated largely unsupervised testing scheme was required to provide standardized measurement conditions and explore a large parameter space (Section 3.2). We measured transient visual responses under open loop conditions by controlling the phase of sine grating stimuli in real time (Section 3.3). Finally, we demonstrate how the open loop paradigm enabled a simple and robust method to analyze the large amounts of acquired behavioral data (Section 3.4). Detailed analyses of behavioral data measured under hundreds of measurement conditions and comprising several 10,000 individual trials will be presented elsewhere (Fry and Rohrseitz, in preparation).

#### 3.2. Process automation

Standardized and automated measurements were performed by inducing single flies to fly near the center of the wind tunnel and then testing them with a precisely defined visual stimulus of 1 s duration. In absence of a fly within the cameras' tracking range, a static sine grating pattern ( $SF = 6.66 \text{ m}^{-1}$ ) was displayed on the side walls of the wind tunnel. A fly flying up wind approached the middle of the wind tunnel, where its position was tracked along a distance of about 0.4 m. We implemented an automated procedure to keep the fly near the middle of the wind tunnel following David's (1982) manual method. We controlled the pattern TF linearly with the fly's up wind position according to:

$$TF = X \frac{-2 \text{ Hz}}{0.2 \text{ m}} \quad (3)$$

where  $X$  is the fly's measured position along the wind tunnel relative to the middle (see Fig. 4 for coordinate system). The corresponding pattern speed is calculated from  $TF/SF$ , with  $SF = 6.66 \text{ m}^{-1}$  (see above). With increasing up wind position the pattern speed was moved with increasing speed in the opposite direction, causing the fly to reduce speed and drift down wind (and vice versa). As a result, the fly was held near the middle of the wind tunnel where it perceived its 'preferred' pattern speed (David, 1982), measured in our wind tunnel at about  $V_{\text{Pref}} = -0.141$  (interquartile range:  $-0.104$  to  $0.137 \text{ m s}^{-1}$ ). Tests were induced under standard conditions as specified by three criteria: (1) time interval after previous test at least 2 s; (2) distance travelled within 0.25 s less than 0.08 m; (3) fly's current position within a cuboid of length 0.2 m, width and height 0.1 m, centered in the wind tunnel. When all three conditions were met a single test was automatically performed, after which the process repeated itself.

#### 3.3. Open loop test trials

A test consisted of a 1 s presentation of a moving sine grating with specified TF and SF during which the fly's 3D position was logged for later analysis (Section 3.4). Numerous other test paradigms were applied, including the use of distorted grating patterns (Section 2.5) and naturalistic images. As they are based on the

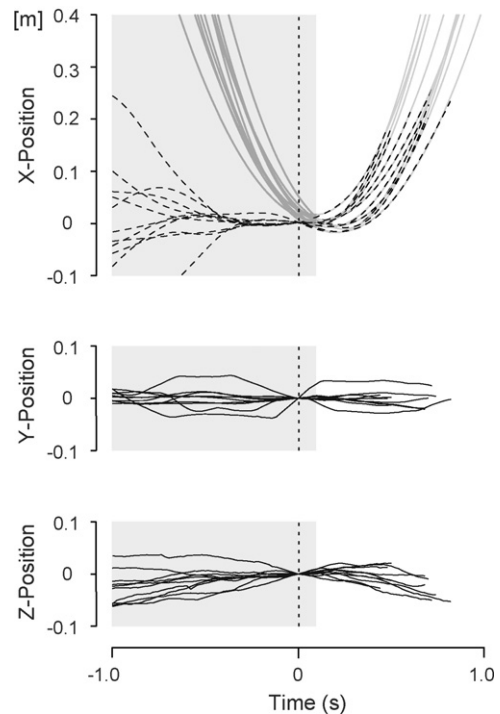


**Fig. 5.** Representative raw data sample. Body position was measured prior to ( $t < 0$ ) and after onset of open loop pattern stimulation (temporal frequency: 4 Hz, spatial frequency  $12.5 \text{ s}^{-1}$ ,  $n = 11$  flights). Mean acceleration of each sample was measured from the fitting parameters of a parabola ( $t > 0.1 \text{ s}$ ;  $n = 11$ ).

same principles these are not further discussed. To maintain a constant TF with respect to the fly's position, the pattern phase was continually adjusted according to the fly's current position along the wind tunnel. In the case that the flies were induced to accelerate in the up wind direction, the body axis direction remained closely aligned with the flight direction, as confirmed by high-speed video analysis (data not shown). Assuming that head movements were small during straight flight, the retinal stimulation can be inferred from the display coordinates (Fig. 4).

As shown in the analysis (Section 3.4), the variance of the data was low compared to typical behavioral measures of free flight behavior. As we did not observe differences between individuals, the data were pooled and treated as independent. In each experimental session, 4 test conditions and a control condition ( $TF = -2 \text{ Hz}$ ,  $SF = 10 \text{ m}^{-1}$ ) were repeated sequentially until sufficient data were acquired.

#### 3.4. Data analysis

##### 3.4.1. Trial evaluation

Representative examples of measured 3D position data are shown in Fig. 5. At time zero, the flies are located near the middle of the wind tunnel ( $X = Y = Z = 0$ ), as required by the hovering criteria (Section 3.2). When stimulated with up wind (regressive) pattern motion ( $TF = 4 \text{ s}^{-1}$ ;  $SF = 12.5 \text{ m}^{-1}$ ), the flies flew up wind ( $X$  position increases). The lateral ( $Y$ ) position remained close to the middle of the wind tunnel ( $Y = 0$ ) with deviations typically well below 0.05 m. Vertical ( $Z$ ) position remained roughly constant, with a slight tendency for the flies to descend. In presence of strong optic flow stimulation, as in the present example, tracking terminated when the fly flew out of the tracking range within the 1 s trial period.

The open loop stimulation resulted in a highly stereotyped response that could be evaluated with a simple and robust

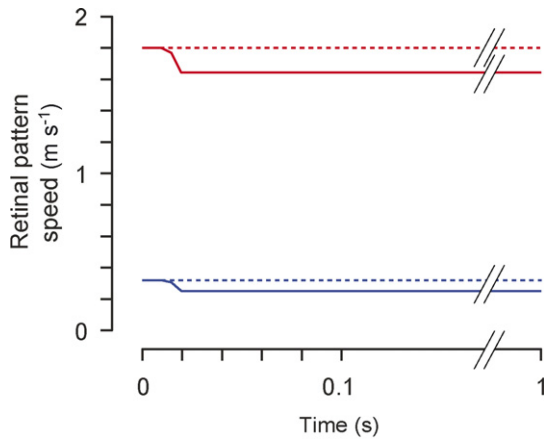


**Fig. 6.** Stimulation error due to system time lag. Programmed retinal slip speeds (stippled lines) of 0.32 (blue) and 1.8 m s<sup>-1</sup> (red) are compared with the effectively perceived speeds (solid lines), as calculated from the average system delay of 0.038 s and the measured time course of the fly's *X* position. For interpretation of the references to colour in this figure legend, the reader is referred to the web version of the article.

procedure. The *X* position after stimulus onset ( $t > 0$ ) was well approximated by fitting a second order polynomial of the form

$$X(t) = a \cdot t^2 + b \cdot t + c \quad (4)$$

The parabolic fit implies that, remarkably, the flies maintained a constant acceleration for the duration of the measurement, which provided a straightforward measure of the transient response strength. The constant acceleration of the fly is explained with a constant slip speed between the fly and the pattern (described in further detail below, also see Fig. 6) and the open loop stimulation procedure. While the fly is 'overtaking' the pattern, the pattern speed increases as to maintain open loop conditions, causing both the fly and the pattern to accelerate. We obtain the body acceleration from the second derivative of Eq. (4):

$$\ddot{X}(t) = 2 \cdot a \quad (5)$$

The mean acceleration is then given by the value of  $2 \cdot a$ .

The occasional presence of several flies in the wind tunnel could lead to invalid flight tracks. These were easily identified from a discontinuity of the position measurements and were subsequently removed from the data pool. Occasional outliers (fewer than 2%) were identified from a *r*-squared value below 0.9 and removed from the analysis.

### 3.4.2. Stimulation error due to system time lag

Assuming a parabolic position function for the fly (Section 3.4.1; Eq. (4); Fig. 5), the pattern phase offset required to perfectly compensate for the fly's changing position (i.e. maintain open loop condition) is given by:

$$\Phi_O(t) = X(t) = a \cdot t^2 + b \cdot t + c \quad (6)$$

In reality, the phase compensation occurs after the system delay  $\tau$ , measured at 0.038 s (Section 2.4), resulting in the actual phase offset:

$$\Phi_{O, \text{Delay}}(t) = X(t - \tau) = a \cdot (t - \tau)^2 + b \cdot (t - \tau) + c \quad (7)$$

Now we can compute the error between the ideal phase and the actual phase (using  $b = c = 0$  for a parabola originating in zero):

$$\Phi_{\text{Error}}(t) = \Phi_O(t) - \Phi_{O, \text{Delay}}(t) = a(2 \cdot t \cdot \tau - \tau^2) \quad (8)$$

The error in pattern speed, relevant to the question posed in our experiments, is the derivative of the phase error:

$$\dot{\Phi}_{\text{Error}}(t) = 2 \cdot a \cdot \tau \quad (9)$$

In our experiments, therefore, the pattern speed error depends only on the system latency  $\tau$  and the fly's measured mean acceleration for a given stimulus. Fig. 6 shows the calculated time course of the programmed (stippled lines) and perceived (solid lines) pattern speeds in the case of a moderate pattern speed (0.32 m s<sup>-1</sup>, blue; same as used in Fig. 5), and a high pattern speed (1.8 m s<sup>-1</sup>, red) that resulted in the maximal measured acceleration. The stimulus error reached a constant value of about 10% of the programmed pattern speed within 0.02 s.

## 4. Discussion

We described methods and concepts that allowed freely flying fruit flies to be stimulated with arbitrary visual stimuli in an automated experimental paradigm. Specifically, the implementation of an automated 'one-parameter open loop' paradigm allowed testing a freely flying fly under realistic free flight conditions, while controlling a single parameter, the horizontal optic flow, in open loop for a detailed characterization of transient speed responses. The described procedures were also applied in experiments using real time pattern distortion; Gabor patches for localized stimulation and stimulation with naturalistic images, described elsewhere (Fry et al., in preparation).

The main features of the developed methodology include: (1) the ability to measure transient response properties under free flight conditions using open loop stimulation, (2) process automation for high data throughput and measurement standardization and (3) simplified data analysis due to highly controlled test conditions. Taken together, our application of VR display techniques in a freely flying insect demonstrates the experimental power of software-controlled experimentation based on virtual reality display technology.

### 4.1. Broader relevance of methods

The relevance of the described methods extends far beyond the present motivation for a detailed system identification approach. The ability to implement powerful experimental paradigms in freely moving animals is met with an increasing demand for interdisciplinary research addressing the functional role of neuromotor pathways under realistic behavioral conditions.

In fruit flies, as in other animal models amenable to genetic techniques, specific cell types can be targeted with high specificity using advanced genetic techniques (review of Gal4-UAS system: Duffy, 2002; restriction techniques; MARCM: Lee and Luo, 1999; FLP/FRT: Golic and Lindquist, 1989; Xu and Rubin, 1993; Stockinger et al., 2005), making the neuromotor pathways amenable to 'genetic dissection' (Heisenberg, 2003; Liu et al., 2006; Rister et al., 2007). This approach depends critically on the ability to perform meaningful quantitative behavioral analyses in a functionally relevant context, the demand for which is rapidly increasing. Likewise in other model systems there is a need for broader behavioral analysis, while providing highly standardized test conditions, including applications in behavioral neurosciences, drug testing, etc.

The profound understanding of biological control principles based on a more rigorous behavioral characterization of sensorimotor control loops is also of direct relevance for the design of biomimetic robots, including MAV. Various forms of bio-inspired robots have been implemented in the past, mainly as experimental platforms (e.g. Webb et al., 2004). Truly biomimetic robotic implementations, however, require highly detailed system analyses of sensorimotor pathways to be performed in freely moving animals (Rohrseitz and Fry, in preparation), to which end the presented methodologies were developed.

#### 4.2. Advantages and limitations of software-based experiment design

The use of general purpose digital hardware requires careful consideration of its limitations. Our setup was limited in two main aspects. First, the significant system latency due to digital processing resulted in a systematic deviation between the actual and desired stimulus conditions. Second, the use of a standard LCD projector resulted in image tearing and spatial aliasing due to limited refresh frequency. While we did not consider these limitations critical for our application, other experimental settings may demand for improved hardware performance, in which case high performance components should instead be used.

Contrasting these limitations, the use of digital electronics provides several clear advantages. First, standard hardware and software solutions are affordable and allow experimental set ups to be more easily replicated than custom-built solutions based on mechanical or analog electronics components. Second, experimental design in software allows increased flexibility, process control, and the ability to create VR stimulus conditions that are impossible to implement with standard hardware solutions.

Given the demand for increasingly sophisticated experimental paradigms for freely moving animals (Section 4.1), the use of general purpose digital hardware and software design promises powerful approaches for behavioral neurosciences, which can complement, rather than replace, existing solutions and paradigms.

#### 4.3. Extension to other experimental contexts

Due to the flexibility of software controlled experimental design, basic concepts of an approach – such as the ‘one-parameter open loop’ paradigm – can be transferred to experimental applications in other species and behavioral contexts. One fundamental requirement to perform similar experiments in other species is the ability to track their position in real time, for which measuring techniques are becoming increasingly available (Reynolds and Riley, 2002). The second requirement is the availability of suitable stimulation techniques, which are also becoming more readily available. In conclusion, the close integration of experimental concepts with the flexible use of measurement, stimulation and analysis techniques opens up new opportunities for behavioral neurosciences.

#### Acknowledgements

The authors thank Jérôme Frei, Marie-Christine Fluet and Martin Bichsel for their contributions to this work. Financial support was provided by the Human Frontiers Science Program, the University of Zürich (to S.N.F.), the Swiss Federal Institute of Technology (ETH-0-20338-06 to N.R.), the National Science Foundation (FIBR 0623527) and the Air Force Office of Scientific Research (FA9550-06-1-0079 to M.H.D.).

#### References

- Baader A. Simulation of self-motion in tethered flying insects: an optical flow field for locusts. *J Neurosci Methods* 1991;38:193–9.
- Baker PS. Flying locust visual responses in a radial wind tunnel. *J Comp Physiol A Neuroethol Sens Neural Behav Physiol* 1979;131:39–47.
- Bender JA, Dickinson MH. Visual stimulation of saccades in magnetically tethered *Drosophila*. *J Exp Biol* 2006;209:3170–82.
- Blondeau J. Aerodynamic capabilities of flies, as revealed by a new technique. *J Exp Biol* 1981;92:155–63.
- Borst A, Bahde S. What kind of movement detector is triggering the landing response of the housefly? *Biol Cybern* 1986;55:59–69.
- Buchner E. Behavioral analysis of spatial vision in insects. In: Ali MA, editor. *Photoreception and vision in invertebrates*. New York: Plenum Press; 1984. p. 561–621.
- Collett T, Nalbach HO, Wagner H. Visual stabilization in arthropods. *Rev Oculomot Res* 1993;5:239–63.
- David CT. Compensation for height in the control of groundspeed by *Drosophila* in a new, ‘barber’s pole’ wind tunnel. *J Comp Physiol A Neuroethol Sens Neural Behav Physiol* 1982;147:485–93.
- David CT. Optomotor control of speed and height by free-flying *Drosophila*. *J Exp Biol* 1979;82:389–92.
- Dickinson MH. The initiation and control of rapid flight maneuvers in fruit flies. *Integr Comp Biol* 2005;45:274–81.
- Duffy JB. GAL4 system in *Drosophila*: a fly geneticist’s Swiss army knife. *Genesis* 2002;34:1–15.
- Fry SN, Bichsel M, Müller P, Robert D. Tracking of flying insects using pan-tilt cameras. *J Neurosci Methods* 2000;101:59–67.
- Fry SN, Müller P, Baumann H-J, Straw AD, Bichsel M, Robert D. Context-dependent stimulus presentation to freely moving animals in 3D. *J Neurosci Methods* 2004;135:149–57.
- Fry SN, Sayaman R, Dickinson MH. The aerodynamics of free-flight maneuvers in *Drosophila*. *Science* 2003;300:495–8.
- Fry SN, Sayaman R, Dickinson MH. The aerodynamics of hovering flight in *Drosophila*. *J Exp Biol* 2005;208:2303–18.
- Frye MA, Dickinson MH. Fly flight: a model for the neural control of complex behavior. *Neuron* 2001;32:385–8.
- Frye MA, Dickinson MH. Motor output reflects the linear superposition of visual and olfactory inputs in *Drosophila*. *J Exp Biol* 2004;207:123–31.
- Gewecke M. Die Wirkung von Luftströmung auf die Antennen und das Flugverhalten der blauen Schmeißfliege (*Calliphora erythrocephala*). *J Comp Physiol A Neuroethol Sens Neural Behav Physiol* 1967;54:121–64.
- Golic KG, Lindquist S. The FLP recombinase of yeast catalyzes site-specific recombination in the *Drosophila* genome. *Cell* 1989;59:499–509.
- Götz KG. Flight control in *Drosophila* by visual perception of motion. *Kybernetik* 1968;4:199–208.
- Götz KG. The optical transfer properties of the complex eyes of *Drosophila*. *Kybernetik* 1965;2:215–21.
- Götz KG. Optomotorische Untersuchung des visuellen Systems einiger Augenmutanten der Fruchtfliege *Drosophila*. *Kybernetik* 1964;2:77–92.
- Götz KG, Wenking H. Visual control of locomotion in the walking fruitfly *Drosophila*. *J Comp Physiol A Neuroethol Sens Neural Behav Physiol* 1973;85:235–66.
- Gray JR, Pawlowski V, Willis MA. A method for recording behavior and multineuronal CNS activity from tethered insects flying in virtual space. *J Neurosci Methods* 2002;120:211–23.
- Hedwig B, Poulet JFA. Complex auditory behaviour emerges from simple reactive steering. *Nature* 2004;430:781–5.
- Heisenberg M. Mushroom body memoir: from maps to models. *Nat Rev Neurosci* 2003;4:266–75.
- Heisenberg M, Buchner E. The rôle of retinula cell types in visual behavior of *Drosophila melanogaster*. *J Comp Physiol A Neuroethol Sens Neural Behav Physiol* 1977;117:127–62.
- Heisenberg M, Wolf R. On the fine structure of yaw torque in visual flight orientation of *Drosophila melanogaster*. *J Comp Physiol A Neuroethol Sens Neural Behav Physiol* 1979;130:113–30.
- Hengstenberg R, Sandeman DC, Hengstenberg B. Compensatory head roll in the blowfly *Calliphora* during flight. *Proc R Soc Lond, B, Biol Sci* 1986;227:455–82.
- Hoy RR, Paul RC. Genetic control of song specificity in crickets. *Science* 1973;180:82–3.
- Juusola M, Hardie RC. Light adaptation in *Drosophila* photoreceptors: I. Response dynamics and signaling efficiency at 25 °C. *J Gen Physiol* 2001;117:3–25.
- Kennedy JS. The visual responses of flying mosquitoes. *Proc Zool Soc Lond A* 1939;109:221–42.
- Land MF, Collett TS. Chasing behaviour of houseflies (*Fannia canicularis*). *J Comp Physiol A Neuroethol Sens Neural Behav Physiol* 1974;89:331–57.
- Lee T, Luo LQ. Mosaic analysis with a repressible cell marker for studies of gene function in neuronal morphogenesis. *Neuron* 1999;22:451–61.
- Liu G, Seiler H, Wen A, Zars T, Ito K, Wolf R, Heisenberg M, Liu L. Distinct memory traces for two visual features in the *Drosophila* brain. *Nature* 2006;439:551–6.
- Lott GK, Rosen MJ, Hoy RR. An inexpensive sub-millisecond system for walking measurements of small animals based on optical computer mouse technology. *J Neurosci Methods* 2007;161:55–61.
- Mayer M, Vogtmann K, Bausenwein B, Wolf R, Heisenberg M. Flight control during ‘free yaw turns’ in *Drosophila melanogaster*. *J Comp Physiol A Neuroethol Sens Neural Behav Physiol* 1988;163:389–99.
- Nalbach G, Hengstenberg R. The halteres of the blowfly *Calliphora*: II. Three-dimensional organization of compensatory reactions to real and simulated rotations. *J Comp Physiol A: Neuroethol Sens Neural Behav Physiol* 1994;175:695–708.
- Pringle JWS. The gyroscopic mechanism of the halteres of Diptera. *Philos Trans R Soc Lond B Biol Sci* 1948;233:347–84.
- Reynolds DR, Riley JR. Remote-sensing, telemetric and computer-based technologies for investigating insect movement: a survey of existing and potential techniques. *Comp Electron Agri* 2002;35:271–307.
- Rister J, Pauls D, Schnell B, Ting CY, Lee CH, Sinakevitch I, Morante J, Strausfeld NJ, Ito K, Heisenberg M. Dissection of the peripheral motion channel in the visual system of *Drosophila melanogaster*. *Neuron* 2007;56:155–70.
- Robertson RM, Johnson AG. Collision avoidance of flying locusts: steering torques and behaviour. *J Exp Biol* 1993;183:35–60.
- Schuster S, Strauss R, Götz KG. Virtual-reality techniques resolve the visual cues used by fruit flies to evaluate object distances. *Curr Biol* 2002;12:1591–4.
- Srinivasan MV, Zhang S. Visual motor computations in insects. *Annu Rev Neurosci* 2004;27:679–96.

- Srinivasan MV, Zhang S, Lehrer M, Collett TS. Honeybee navigation en route to the goal: visual flight control and odometry. *J Exp Biol* 1996;199:237–44.
- Stark WS, Johnson M. Microspectrophotometry of *Drosophila* visual pigments: determinations of conversion efficiency in R1-6 receptors. *J Comp Physiol A: Neuroethol Sens Neural Behav Physiol* 1980;140:275–86.
- Stockinger P, Kvitsiani D, Rotkopf S, Tirian L, Dickson BJ. Neural circuitry that governs *Drosophila* male courtship behavior. *Cell* 2005;121:795–807.
- Straw AD, O'Carroll DC. Motion blur applied to eliminate artifacts in apparent motion displays. *J Vis* 2003;3:782.
- Straw AD, Warrant EJ, O'Carroll DCA. 'Bright zone' in male hoverfly (*Eristalis tenax*) eyes and associated faster motion detection and increased contrast sensitivity. *J Exp Biol* 2006;209:4339–54.
- Taylor GK, Zbikowski R. Nonlinear time-periodic models of the longitudinal flight dynamics of desert locusts *Schistocerca gregaria*. *J R Soc Interface* 2005;2:197–221.
- Webb B, Harrison RR, Willis MA. Sensorimotor control of navigation in arthropod and artificial systems. *Arthropod Struct Dev* 2004;33:301–29.
- Willis MA, Arbas EA. Odor-modulated upwind flight of the sphinx moth, *Manduca sexta* L. *J Comp Physiol A Neuroethol Sens Neural Behav Physiol* 1991;169:427–40.
- Xu T, Rubin GM. Analysis of genetic mosaics in developing and adult *Drosophila* tissues. *Development* 1993;117:1223–37.